Improving Signal-Strength-based Distance Estimation in UWB Transceivers

Leo Botler
Institute for Technical Informatics
Graz University of Technology
Graz, Austria
leo.happbotler@tugraz.at

Konrad Diwold
Institute for Technical Informatics
Graz University of Technology
Graz, Austria
kdiwold@gmail.com

Kay Römer
Institute for Technical Informatics
Graz University of Technology
Graz, Austria
roemer@tugraz.at

ABSTRACT

Ultra-wideband (UWB) technology has become very popular for indoor positioning and distance estimation (DE) systems due to its decimeter-level accuracy achieved when using time-of-flight-based techniques. Techniques for DE relying on signal strength (DESS) received less attention. As a consequence, existing benchmarks consist of simple channel characterizations rather than methods aiming to increase accuracy. Further development in DESS may enable lower-cost transceivers to applications that can afford lower accuracies than those based on time-of-flight. Moreover, it is a fundamental building block used by a recently proposed approach that can enable security against cyberattacks to DE which could not be avoided using only time-of-flight-based techniques. In this paper, we aim to benchmark the performance of machine-learning models when used to increase the accuracy of UWB-based DESS. Additionally, aiming for implementation in commercial off-the-shelf (COTS) transceivers, we propose and evaluate an approach to resolve ambiguities compromising DESS in these devices. Our results show that the proposed DE approaches have sub-decimeter accuracy when testing the models in the same environment and positions in which they have been trained, and achieved an average MAE of 24 cm when tested in a different environment. 3 datasets obtained from our experiments are made publicly available.

KEYWORDS

UWB, Signal strength, RSSI, Machine Learning, Ambiguity

ACM Reference Format:
Leo Botler, Konrad Diwold, and Kay Römer. 2023. Improving Signal-Strength-based Distance Estimation in UWB Transceivers. In *Cyber-Physical Systems and Internet of Things Week 2023 (CPS-IoT Week Workshops '23), May 9–12, 2023, San Antonio, TX, USA.* ACM, New York, NY, USA, 6 pages. https://doi.org/10.1145/3576914.3587519

1 INTRODUCTION

Accurate distance estimation (DE) is an enabler for several applications, including Passive Keyless Entry and Start (PKES), and Indoor Positioning Systems. DE can be currently achieved with sub-decimeter accuracy by commercial off-the-shelf (COTS) time-of-flight (ToF)-based ultra-wideband (UWB) transceivers [8].

DE approaches relying on UWB's received signal strength (RSS) have been less explored. Typical approaches make use of a single feature of the signal, namely the first-path amplitude of the signal reaching the receiver, and characterize the error based on its standard deviation.

In this paper, we benchmark the accuracy of machine learning (ML) regressors for DE based on RSS-related features using UWB transceivers, and we show that these methods improve the accuracy achieved by the state-of-the-art approach. To our knowledge, this is the first time that ML is applied to UWB-based DE relying on signal strength (DESS). We do not aim to achieve more accurate estimations than those achieved by ToF-based transceivers.

Moreover, we investigate and propose a solution to the problem of ambiguous estimations affecting COTS transceivers, explained in Subsection 2.4. In general, experiments making use of laboratory equipment differ from those using COTS devices in the sense that they 1) afford a higher and more stable sampling frequency, 2) do not use an automatic gain control (AGC) stage in the receiver - which will be shown in Section 4 to be critical - and, 3) make use of wider bandwidths than those allowed by standards, which directly impacts the accuracy of distance estimations.

Two factors motivate us to investigate DESS:

(1) It may lead to the development of simpler UWB transceivers featuring lower costs and sampling rates than those using ToF [5]. These can be useful in applications affording accuracies up to a few decimeters. Throughout our experiments, we opted for sticking to the IEEE 802.15.4-2011 standard [2] aiming to create alternatives that could serve as an extension to this standard rather than creating an incompatible approach, e.g., occupying the entire spectrum reserved for this technology.
(2) We recently showed that the *Distance Enlargement Fraud* - a particular attack on DE which cannot be overcome solely by using ToF measurements - can be detected or limited by using a novel framework relying on hybrid ToF and RSS distance estimations [7]. In this attack, a malicious entity P tries to convince another entity V performing DE to it that they are further away than they really are. While in a ToF-based system P performs the attack by inserting a time delay in the response time, in a RSS-based system P can amplify signals or communicate different power levels than those received, making this attack challenging to overcome. Our approach imposes bounds to those time delays and power gains by letting V check a set of geometrical constraints.

CPS-IoT Week Workshops '23, May 9–12, 2023, San Antonio, TX, USA

ACM ISBN 979-8-4007-0049-1/23/05.
https://doi.org/10.1145/3576914.3587519

As UWB transceivers using ToF currently achieve DE with decimeter-level accuracy, the practicality of our approach is limited by the accuracy of RSS distance estimations obtained when using standard-compliant UWB radios.

The main contributions of this paper are:

- We propose and benchmark the accuracy of ML regressors (54 in total) to perform DESS using UWB. The best model found achieved DE with accuracy as low as 24 cm in unknown environments, more than doubling the state-of-the-art accuracy [5].
- We generate 3 datasets stemming from real-world experiments using COTS devices, incorporating a set of parameters and features not found in the public domain. In order to support future research on this topic, we make our datasets publicly available;
- Based on the observation that the transceivers' intrinsic non-linearity severely compromises DESS accuracy, we propose and evaluate a method to increase the accuracy of DESS on COTS UWB transceivers. The effectiveness of the proposed method is supported by experimental data.

2 APPROACH AND METHODS

In this section, we explain how UWB and ML technologies are utilized to estimate distance, introduce the features utilized, and give an overview of the ambiguity issue affecting DESS on COTS transceivers.

2.1 Background on UWB Technology

Due to the short pulse duration (≈2 ns), UWB technology enables the receiver to separate in time the signal received through the first path from the multipath reflected signals. A channel estimation, also known as channel impulse response (CIR), is used by UWB receivers to accurately determine the point in time when a transmitted pulse first reaches the receiver. To this end, a leading edge detection algorithm is typically applied on the absolute value of the CIR, whose samples are proportional to the power of the received signal, but, in COTS devices, are normalized, as will be discussed.

In our experiments, we use the DW1000 [8] transceiver, which provides a CIR estimation by sampling the baseband received signal at a rate of ≈1 GSPS, and storing 1015 complex (1015 real + 1015 imaginary) CIR samples in memory. Those can be retrieved from the transceiver. Several examples of plots of absolute values of different CIRs can be seen in Figure 1, where the X-axis' dimension is *time*, with a 1 ns interval between samples, and the Y-axis is proportional to the amplitude of the received signal. We use only 32 out of the 1015 samples stored, as later samples were found to contain little power in the scenarios tested. Reducing the number of samples decreases the complexity of our models. Note that the CIR itself contains no information about the time of arrival of the signal. This is stored in other registers, which are ignored in this paper.

2.2 ML-Based Approach for DE and Regressors

The decay of UWB's RSS has been modeled in the literature as a log-normal path-loss equation [5]. One can use such models for DE given an RSS-related feature. Instead of using a single feature, ML models are capable of combining several features and, in many cases, achieve more accurate estimations. Additionally, several ML models are capable to capture non-linear behaviors in the data, which can be hard to represent using analytical equations.

Table 1: List of acronyms of features acquired.

Abbreviation	Term
FPPL	First Path Power Level
RSSI	Received Signal Strength Indicator
FP_IDX	First Path Index
LDE_PPAMPL	Leading Edge Peak Path Amplitude
LDE_PPINDX	Leading Edge Peak Path Index
FP_AMPLX	First Path Amplitude Point X, X $\in \{1, 2, 3\}$
CIRX	Absolute value of CIR sample X, X $\in \{1 \dots 32\}$

To train and test ML models, we use data collected from the transceiver at known locations. The separation distance at each location serves as ground truth values. After the training phase, the ML models are tested by estimating distances using the same features used for training, but different samples.

As our target variable is continuous, we are interested in *regression* models (opposed to classification models), which can provide as an output continuous DE values. This enables estimating distances at a finer granularity than the 0.5 m distance step size used in our experiments - typically too coarse for UWB DE.

Our analyses include several families of regressors classified according to [11] as: linear and generalized linear models, LASSO and ridge regression, Bayesian models, Gaussian processes, nearest neighbors, regression trees and rules, random forests, bagging and boosting and support vector regression.

All ML models are trained and tested in two different environments. While testing the models in the same environment where they have been trained provides an upper bound on the expected DE accuracy, testing them in a different environment enables us to check how well they generalize. Aiming to assess the information provided by the transmission power gain, we train k-Nearest Neighbors regressors in 2 different ways. First, we use as features the absolute values of the 32 CIR samples extended with the TX power gain, which is deterministic. Next, we remove the power gain from the feature set to compare with the results from the previous approach; the accuracy should vary according to the level of information provided by this feature. These results should indicate whether to include the power gain in the feature set, and are detailed in Subsections 4.2 and 4.3. This is essential for benchmarking the regressors, which is detailed in Subsection 4.4. In this step, we assess the performance of 54 out of the 55 regressors implemented in *scikit-learn* [16] version 1.0.2[1] using their default parameters. The complete list of regressors can be found in [16].

2.3 Features

The set of features that we use is intentionally selected to reflect only the RSS. The features used are taken from [9] and listed in Table 1. They are all calculated by the transceiver and stored in registers, except for the absolute values of CIR samples whose complex values are stored.

[1]Quantile Regressor was excluded from this analysis for requiring an extremely high training overhead.

We use the FPPL feature to train and test our simplest models, discussed in Subsection 4.1. The FPPL is a scalar value calculated using 3 samples in the vicinity of the first peak path, and is, therefore, proportional to the power of this peak. Thus, the power from the reflected signals, which typically misleads power-based DE, has a less severe impact than when using other metrics, such as the RSSI. This result is presented in [5] and was confirmed by our experiments, but is not detailed in this paper.

In an attempt to improve the results obtained with the FPPL, we use the 32 absolute values of CIR samples as features, on top of which the other features can be calculated. The CIR contains information about the environment due to the reflected signals, which, in principle, do not interfere with the first-path signal.

2.4 Approach for Resolving Ambiguous Estimations

The DW1000 features an AGC stage in its front end. AGCs are common in wireless receivers and enable longer communication ranges by amplifying the received signal. It aims to normalize the signal's amplitude by applying a low-magnitude gain to high-power signals and vice-versa. Thus, using the previously mentioned CIR samples without accounting for the gain applied by the AGC makes DESS difficult, if not meaningless.

As illustrated in Figure 1 a), the RX should always saturate regardless of its distance to the TX when the AGC is turned on, leading to *ambiguous* CIR estimations, i.e., a single CIR amplitude is associated with multiple TX-RX distances. This issue may be mitigated by turning the AGC off, as illustrated in plot b). However, even in this case, the RX can saturate. This should occur at shorter TX-RX distances and high TX powers, and reduces the probability for the RX to correctly discriminate between distances. In this case, transmitting at lower power levels may resolve the ambiguity issue as each CIR amplitude is associated with a unique distance, as illustrated in plot c) of the same figure. This simple approach to resolve ambiguities will be thoroughly evaluated in Section to find optimum features and models, leading to a method that can improve RSS-based DE.

3 EXPERIMENTS

This section describes 3 experiments that we designed to assess the performance of UWB DESS with the goals of:

- E.I) checking the influence of the AGC on RSS measurements obtained with the DW1000 [9];
- E.II) testing the capability of estimating distances using only RSS-related features to train ML models in a known environment. No ToF-related feature is utilized;
- E.III) evaluating how the previously obtained models generalize, i.e., can perform DE in a different environment from the one it was trained in without any re-calibration.

To achieve goal E.I), we repeat one experiment twice in the same environment (a building hallway), initially with the AGC turned on, and then with it turned off. In both rounds, 2 COTS UWB modules (TX and RX) were placed facing each other at different distances while TX transmits signals at different power levels to RX. These experiments also enable us to achieve goal E.II). In order

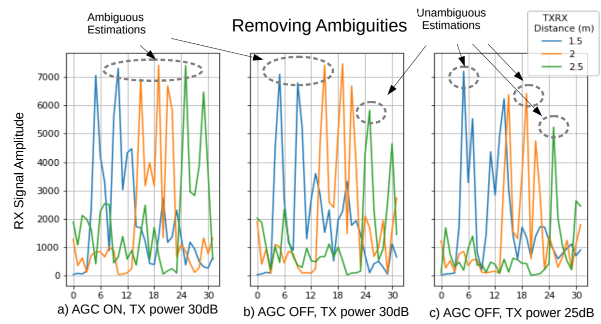

Figure 1: Plots of absolute values of selected CIRs samples at 3 different distances. The CIRs corresponding to TXRX distances of 2 m **and** 2.5 m **are shifted in time (x-axis) to facilitate visualization. All received signals have the same amplitude in plot a), which illustrates signals received using the AGC on at a high transmission power. In b), the furthest distance signal has a lower amplitude than the other, as a consequence of turning the AGC off. Plot c), obtained with AGC off and a lower transmission power shows all the signals having different amplitudes.**

to achieve goal E.III), we perform the last experiment in a different environment.

Hardware and Parameters: For all our experiments we used the DWM1003 module as TX, which is an evaluation module from Decawave, embedding a single DW1000 chip [8]. As RX, we used a DWM1002 module [10], which contains 2 DW1000 chips clocked by the same source, connected each to a dedicated antenna. The two antennas are separated by a distance of ≈2.05 cm. Every packet transmitted was acquired by the two chips, and all packets correctly received by both chips were added to our dataset. For simplicity, we use data from a single receiver chip throughout our analysis.

The experiments used Channel 7 from the standard (center frequency=6489.6 MHz, bandwidth= 1081.6 MHz), clear line-of-sight (LOS) between transceivers, and the 68 different programmable power gains $\in \{0\ dB, 0.5\ dB, ..., 33.5\ dB\}$ available in the DW1000, which we consider sufficient to provide a rich feature set. Other parameters were kept as default according to [1].

3.1 Experiment in a hallway with AGC turned on

This experiment was conducted in a ≈1.9 m wide hallway. The modules were placed approximately 1.5 m above the floor and oriented along the length of the hallway with antennas facing each other. Their separation distance was varied from 0.5 m to 6.5 m in steps of 0.5 m. This was found to be the maximum communication distance at maximum transmission power when the receiver's AGC was **turned off**. Distances were measured with a measuring tape so that errors in the range of centimeters are possible. For each distance, a minimum of 1088 (= 16 × 68) packets were transmitted, in such a way that at least 16 packets were transmitted using each of the 68 power gains. The receiver's AGC was **turned on**. The features acquired are independent of ToF and include:

- fppl, rssi, the fp_idx, lde_ppampl, lde_ppindx, fp_ampl1, fp_ampl2 and fp_ampl3. Please, refer to Table 1 for a description of these acronyms and to [9] for an explanation of their physical meaning;
- 32 complex CIR samples, where the 5th sample corresponds to the first peak detected;
- the power gain value used by the transmitter.

3.2 Experiment in a hallway with AGC turned off

We repeat the experiments from Section 3.1, but with the receiver's AGC turned off. Please, notice that, in this experiment, many of the transmitted packets do not reach the receiver, depending on their power gain and on the communication distance. Although it limits the communication range, eliminating the AGC enables us to simply establish an upper bound on the expected accuracy to be achieved using the proposed methods in case the gains provided by the AGC can be obtained or estimated.

3.3 Experiment in a hall with AGC turned off

We repeat the experiments from Section 3.2, but in a wider (≈9.3 m x 5 m) building hall furnished only with working desks and chairs. The reason why the AGC was turned off in this experiment will be clarified in Subsection 4.1.

DATASETS

Separate datasets were generated for each of the experiments 3.1 to 3.3 and can currently be found on [6], along with instructions on how to use them, as well as a description of the available features, which are not restricted to the ones used in our analysis.

4 ANALYSIS AND RESULTS

In this Section, we analyze the approach introduced in Section 2 using the data previously obtained. The metric used to quantify accuracy is the mean absolute error (MAE) obtained per distance and then averaged over all distances, so that the final metric is not dominated by distances with greater sample sizes. MAE was preferred over root mean square error (RMSE) as it equally weighs errors at different distances. Nonetheless, RMSE is occasionally used to enable direct comparisons with existing results using this metric. Additionally, our analyses include measures of memory and processing overhead for both training and testing the models.

4.1 AGC On Vs AGC Off

In order to achieve DE with optimum accuracy using only RSS-related features from the DW1000, we first evaluated how the AGC stage of the transceiver affects the accuracy of estimations. Using data from experiments 3.1 and 3.2, we show in Figure 2 a scatter plot of the FPPL feature over distance for different transmitted power levels. Please, recall that both experiments took place in the same environment, at the same fixed positions.

From this figure, it is clear that, at the distance range observed, the impact of distance on FPPL is higher when the AGC is off. In other words, it is easier to distinguish among distances estimated using this metric due to a reduced overlap of samples obtained at

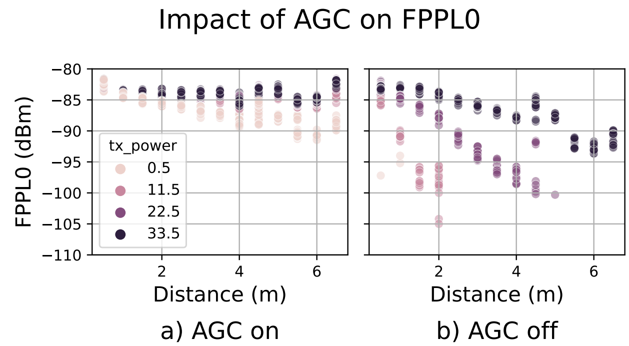

Figure 2: Scatter plot of FPPL over distance in the hallway with AGC turned on a) and off b) for 4 different transmission power gains.

different distances at a given power gain. In order to quantify this result, we evaluate the MAE of the K-Nearest Neighbors (KNN) regressor using the default parameters from [16] version 1.0.2. We used 75 % and 25 % of the data for training and testing, respectively. When using only the maximum transmission power, the averaged MAE decreased from 1.421 m when the AGC is turned on to 0.413 m when it is turned off, showing the benefit of turning the AGC off due to the effect illustrated in Figure 1 b). To further reduce ambiguities, we repeat the previous analysis over all transmission powers tested, resulting in an MAE reduction from 1.282 m when the AGC is turned on to 0.190 m when it is turned off, as illustrated in Figure 1 c). The accuracy is improved by **more than 1m**.

This result can be justified as 1) the role of the AGC is to mitigate the effect of power attenuation over distance, which counteracts the physical principle explored, and 2) in the vicinity of the receiver, the high gain provided by the AGC combined with high TX powers saturates the received signal, generating ambiguous measurements, as shown in Figure 1 a). This effect is attenuated when the AGC is turned off, as shown in Figure 1 b). Finally, the remaining ambiguities - due to the saturation of the receiver even when the AGC is off - can be mitigated by using lower power gains (as in c)).

Having demonstrated the advantages of having the AGC turned off, we utilize only datasets obtained with AGC off in the remaining analyses. Those datasets stem from experiments 3.2 and 3.3.

We highlight that the mean standard deviation of the FPPL feature over all samples obtained in the hall grouped by distance and transmit power was $0.636dB$, which is very close to the value (of $0.64dB$) reported in [5]. Therefore, the current approach alone does not improve DE accuracy compared with the state-of-the-art approach. In fact, it is intended to enable DESS on COTS.

4.2 Using CIR Samples as Features

Further CIR peaks tend to be more attenuated than the first one (proportional to the FPPL), which can provide additional information to the models. Therefore, we evaluate the performance of using as a feature set the absolute values of the 32 complex CIR samples extended by the power gain. We proceed as in Subsection 4.1[2], observing that we also vary the training and testing environment to

[2]From now on, our models use only 2 neighbors and weight points based on the inverse of the distance. All features besides the power gain are standardized by removing the mean and scaling to unity variance.

Table 2: Average MAE values in meters when training a model and testing in 2 different environments, including the power gain in the feature set.

Training Set \ Test Set	Hall	Hallway
Hall	0.032	0.512
Hallway	0.449	0.045

assess the robustness of the models against multipath interference, i.e., how each model generalizes. The results are summarized in Table 2.

We see that when the training and testing environments are the same, the average MAE is limited to a few centimeters, while when testing the model in a different environment than the one it was trained in, the MAE is in the order of half a meter. Therefore, it is possible to recommend such an approach for fingerprinting-based applications requiring high accuracy. This first result already improves the one from Subsection 4.1 with AGC off by ≈16 cm. Furthermore, we can conclude that environments with different multipath characteristics require a training phase, i.e., the proposed model does not generalize well. For future reference, we refer to the current approach as the *standard approach*. The sub-decimeter accuracy obtained is a consequence of overfitting, as the CIRs are stable and sensitive to the environment.

Testing in the hall the FPPL models from Subsection 4.1 - which were trained in the hallway - we get an average MAE of ≈0.28 m, which is even better than the results obtained in this section. Furthermore, as the FPPL may saturate at lower distances and/or higher power gains, we should expect lower power gains to reduce ambiguity and further improve accuracy. In fact, when using only the lowest power gain within the communication range with each distance in the training set, we improve the average MAE to ≈0.24 m. This result **more than doubles the accuracy achieved by the state-of-the-art approach** (of 0.52 m). To find the minimum power gain, we consider transmitting a sounding packet at a high power gain, enabling a rough DE, followed by a second transmission at the coarsely estimated minimum power gain.

It is important to mention that the accurate results from Table 2 were obtained when testing samples at distances already *seen* by the model. If we remove all the samples at a given distance d_i from the training phase, train the model with all the distances $d_j \neq d_i$, and test samples only at this particular *unseen* distance d_i, repeating the procedure for every distance in our experiment, we obtain an average MAE of 0.642 m in the hall and 0.730 m in the hallway, meaning that the accuracy depends on the positions seen by the model and drastically deteriorates when the receiver is located at a position different from those at which the model has been trained. This procedure is known as "k-Fold cross-validation with non-overlapping groups".

The time spent to train this model using a total of 11318 samples was measured to be 2.392 ms while the time spent to predict the entire test set containing 3773 samples was 2.400 s resulting in an average prediction time per sample of ≈636 µs. Those measurements were executed using libraries already mentioned on an Intel® Core™ i7-9850H CPU @ 2.60GHz running Microsoft Windows Version 10.0.19042 Build 19042. The models obtained in the hall and in the hallway occupy 3007 kbytes and 1815 kbytes in memory, respectively.

4.3 Discarding Power Gain

In the previous subsection, we included the power gain used by the transmitter as a feature to train and test the obtained models without showing if there is a benefit of doing it. In this subsection, we remove it from the feature set. As a matter of fact, not transmitting this information reduces the complexity of the DE protocol. Table 3 summarizes the results.

Table 3: Average MAE values in meters when ignoring the knowledge of the transmission power gain.

Training Set \ Test Set	Hall	Hallway
Hall	0.051	1.058
Hallway	0.741	0.057

As expected, all MAEs increased, especially when testing the model in a different environment than the one it was trained in. This result indicates that the knowledge of the transmit power is beneficial (if not critical) for approaches relying on different transmit powers. To our knowledge, this is the first time that such an approach is proposed for UWB. However, this feature is less critical when training and testing the models in the same environment, as the errors are still within decimeter range.

4.4 Other Regressors

Finally, the *standard approach* was tested using other regressors.

KNeighbors shows to be the best regressor achieving an MAE of 2.1 cm when training and testing the model in the same environment. Otherwise, it can be outperformed even without tuning of parameters.

5 RELATED WORK

Two modulation schemes are defined for UWB: pulse-based modulation, which targets low data rate applications, and Orthogonal Frequency Division Modulation (OFDM), which targets high data rate applications. In [18] and [19], the authors evaluated the accuracy achieved with RSSI for OFDM UWB (high data rate). This is not the most obvious approach, as multipath fading should be mostly mitigated when using short pulses in time, which is achieved with pulse-based modulation. The authors characterized channel 15 based on RSSI measurements over a distance of only 2 m and reported mean *positioning* errors in the range of 10 cm to 30 cm. Similarly, we include analyses using the first-path power level (FPPL) instead of the RSSI, and we use COTS transceivers supporting pulse-based modulation. We present expected errors for *DE* rather than for positioning. The latter depends on the number of anchors (devices at known positions) used, as well as on the used positioning algorithms.

In [5], the authors made use of UWB signal statistics for estimating distances. The accuracy of the approach is determined by the standard deviation of an - empirically obtained - Gaussian noise term in the log-normal path-loss equation. The best accuracy is achieved under LOS and equals 0.52 m, which, as shown in Section 4, could be improved down to 0.021 m when using our approach in a known environment, and down to 0.24 m even in unknown environments. Furthermore, the authors used in their experiments a Gaussian pulse generator with a 20 ps duration, which is much shorter than the ≈2 ns standard compliant pulses, used in our experiments. Similarly, in [13] and [12], the authors showed path loss curves from experiments using the same setup as above. The former focused on modeling the UWB channel while the latter evaluated *positioning* errors.

In [17], the UWB channel is characterized using a vector network analyzer (VNA) occupying the whole 7.5 GHz UWB FCC spectrum. Likewise, a VNA was used in [4] for performing UWB measurements in 4 different environments, with bandwidths of 500 MHz and 3 GHz. Both obtained parameters for a log-normal path-loss model, but did not provide an approach to improve DE accuracy.

ML has been recently proposed to improve distance and position estimations. In [14], it was used to improve ToF DEs down to 1.6 cm RMSE in LOS conditions, using a set of features from 3 packets composing a dual-sided two-way ranging (DS-TWR) exchange. Our method requires a single packet instead and no ToF-related information. Furthermore, a similar approach has been proposed in [3] to increase RSS-based DE using BLE technology instead. However, the benefit observed when including the power gain as feature was not justified. This gap is covered in this paper. Additionally, our explanation hints for using the AGC gain as additional feature. The reader should notice that shadowing is much more severe for BLE than for UWB in such a way that models and features suitable for RSS-based BLE DE may not be suitable for UWB.

Many other approaches have been proposed aiming to correct ToF-based ranging estimations, such as [15]. To our knowledge, the use of ML methods has not been used to enable RSS-based UWB DE, which is the gap covered in this paper.

6 CONCLUSIONS AND FUTURE WORK

In this paper, we benchmarked the performance of several ML regressors for the purpose of UWB DE using only RSS-related features. Additionally, we investigated and proposed a solution to issues associated with its implementation on COTS transceivers. Successive analyses enabled finding more suitable parameters, features and regressors to this end.

By using multiple transmit powers, we managed to achieve DE with an accuracy of **24 cm** in an *unknown* environment. This was achieved using the KNN regressor using only the FPPL and the power gain in the feature set. This result **more than doubles** the accuracy achieved by the state-of-the-art approach. The best accuracy achieved with the evaluated regressors in a *known* environment was as high as **2.1 cm**, which was obtained using the same regressor but using the 32 CIR samples in addition to the power gain in the feature set.

Challenges found include setting and reading the AGC parameters of the transceiver - especially, turning the AGC off and reading the AGC gain - as these operations are not available to the users, and tuning the parameters of ML models. Additionally, as lower-complexity transceivers are not available in the market, we used the DW1000 transceiver in our experiments.

Future work includes preprocessing the received signal, using different ML models, tuning the models' parameters, and repeating the experiments and analyses using lower-complexity transceivers. Increasing the communication range of the proposed approaches by using the AGC gain as a parameter instead of turning it off may also be an interesting research direction. We also believe that conducting more experiments, for instance, subject to obstructed LOS between transceivers, would encourage and enable the search towards better DE methods.

ACKNOWLEDGMENTS

This work has been supported by the FFG, Contract No. 881844: "Pro^{2}Future" and the TU Graz LEAD project Dependable Internet of Things.

REFERENCES

[1] 2022. UWB-core. https://github.com/decawave/uwb-core. Accessed: 2022-03-24.

[2] 802.15.4-2011 2015. *IEEE Standard for Low-Rate Wireless Networks.* Standard. The Institute of Electrical and Electronics Engineers, Inc., New York, USA.

[3] Mimonah Al Qathrady and Ahmed Helmy. 2017. Improving BLE distance estimation and classification using TX power and machine learning: A comparative analysis. In *Proceedings of the 20th ACM International Conference on Modelling, Analysis and Simulation of Wireless and Mobile Systems.* 79–83.

[4] N Alsindi, B Alavi, and K Pahlavan. 2007. Empirical pathloss model for indoor geolocation using UWB measurements. *Electronics Letters* 43, 7 (2007), 370–372.

[5] Giovanni Bellusci, Gerard J. M. Janssen, Junlin Yan, and Christian C. J. M. Tiberius. 2008. Low complexity ultra-wideband ranging in indoor multipath environments. In *2008 IEEE/ION Position, Location and Navigation Symposium.* 394–401. https://doi.org/10.1109/PLANS.2008.4570095

[6] Leo Botler. [n. d.]. UWB RSS Dataset. https://bitbucket.org/leobotler/uwb-rss-dataset. Accessed: 2022-04-19.

[7] Leo Botler, Konrad Diwold, and Kay Römer. 2021. A UWB-Based Solution to the Distance Enlargement Fraud Using Hybrid ToF and RSS Measurements. In *Proceedings - 2021 IEEE 18th International Conference on Mobile Ad Hoc and Smart Systems, MASS 2021.* IEEE Publications, 324–334. https://doi.org/10.1109/MASS52906.2021.00049

[8] Decawave. 2015. *DW1000 IEEE802.15.4-2011 UWB Transceiver datasheet.* Decawave Ltd.

[9] Decawave. 2017. *DW1000 User Manual.* Decawave Ltd.

[10] I. Dotlic, A. Connell, H. Ma, J. Clancy, and M. McLaughlin. 2017. Angle of arrival estimation using decawave DW1000 integrated circuits. In *2017 14th Workshop on Positioning, Navigation and Communications (WPNC).* 1–6.

[11] Manuel Fernández-Delgado, Manisha Sanjay Sirsat, Eva Cernadas, Sadi Alawadi, Senén Barro, and Manuel Febrero-Bande. 2019. An extensive experimental survey of regression methods. *Neural Networks* 111 (2019), 11–34.

[12] Thomas Gigl, Gerard J.M. Janssen, Vedran Dizdarevic, Klaus Witrisal, and Zoubir Irahhauten. 2007. Analysis of a UWB Indoor Positioning System Based on Received Signal Strength. In *2007 4th Workshop on Positioning, Navigation and Communication.* 97–101. https://doi.org/10.1109/WPNC.2007.353618

[13] Zoubir Irahhauten, Gerard J.M. Janssen, Homayoun Nikookar, Alex Yarovoy, and Leo P. Ligthart. 2006. UWB Channel Measurements and Results for Office and Industrial Environments. In *2006 IEEE International Conference on Ultra-Wideband.* 225–230. https://doi.org/10.1109/ICU.2006.281554

[14] Julian Walter Karoliny. 2020. *Machine Learning Approaches for High Accuracy Network Localization with UWB/submitted by Julian Karoliny.* Ph. D. Dissertation. Universität Linz.

[15] Peter Krapež, Matjavz Vidmar, and Marko Munih. 2021. Distance Measurements in UWB-Radio Localization Systems Corrected with a Feedforward Neural Network Model. *Sensors* 21, 7 (Mar 2021), 2294. https://doi.org/10.3390/s21072294

[16] F. Pedregosa, G. Varoquaux, A. Gramfort, V. Michel, B. Thirion, O. Grisel, M. Blondel, P. Prettenhofer, R. Weiss, V. Dubourg, J. Vanderplas, A. Passos, D. Cournapeau, M. Brucher, M. Perrot, and E. Duchesnay. 2011. Scikit-learn: Machine Learning in Python. *Journal of Machine Learning Research* 12 (2011), 2825–2830.

[17] Lorenzo Rubio, Juan Reig, Herman Fernández, and Vicent M. Rodrigo-Peñarrocha. 2013. Experimental UWB Propagation Channel Path Loss and Time-Dispersion Characterization in a Laboratory Environment. *International Journal of Antennas and Propagation* 2013 (31 Mar 2013), 350167. https://doi.org/10.1155/2013/350167

[18] A. Waadt, A. Burnic, D. Xu, C. Kocks, S. Wang, and P. Jung. 2010. Analysis of RSSI based positioning with multiband OFDM UWB. In *2010 Future Network Mobile Summit.* 1–8.

[19] S. Wang, A. Waadt, A. Burnic, D. Xu, C. Kocks, G. H. Bruck, and P. Jung. 2010. System implementation study on RSSI based positioning in UWB networks. In *2010 7th International Symposium on Wireless Communication Systems.* 36–40.